Environment. Technology. Resources. Rezekne, Latvia
Proceedings of the 14th International Scientific and Practical Conference. Volume 3, 328-333

Application of a Finite Element Model to Obtain the Influence of the Treatment's Power, Reflecion and Focal Diameter in Laser Texturing of Aluminum

Lyubomir Lazov
Faculty of Engineering
Rezekne Academy of Technologies (RTA)
Rezekne, Latvia
lyubomir.lazov@rta.lv

Ivo Draganov
Faculty of Mechanical and Manufacturing Engineering
University of Ruse
Ruse, Bulgaria
iivanov@uni-ruse.bg

***Abstract*. In this work, a numerical model of laser texturing is considered. A finite element model of a representative sample of pure aluminum was created. The impact of a laser pulse was simulated, assuming a Gaussian volume distribution of the heat flux. Material properties are assumed to be constant and latent heat is accounted for. Results are obtained for the thermal field and the width of the vaporized zone, assuming that the crater is characterized by its maximum width. The numerical model was used to study the influence of pulse power density, reflection, focal diameter and pulse duration. The ablation threshold at different laser pulse durations was determinate.**

Keywords: ***laser texturing, pure aluminum, finite element method (FEM), vaporized zone.***

I. INTRODUCTION

Laser texturing is pulsed processing by means of a laser beam, in which ablation of the material occurs in the impact zone. By multiple repetition of this process, along a predetermined trajectory, a groove is obtained. The industrial application of laser texturing is most often done by creating a number of grooves close enough together to be perceived as a uniform area. Different modifications of the processing sequence is discussed in [1].

Laser texturing serves to improve adherence, wettability, electrical and thermal conductivity, and friction [2]. This application of laser ablation is characterized by an overlap factor less than one and a different diameter of the laser beam, and hence a different size of the resulting crater.

The obtained result depends on the characteristics of the laser machine: scanning speed, repetition rate, average power, laser beam spot, diameter, and pulse duration. Fiber lasers [3], YAG [4] and others are suitable for laser texturing. The duration of the impact varies widely, using nanosecond [5], picosecond [6] and femtosecond lasers [7], [1].

Laser texturing is applicable to various materials, such as metals and their alloys, superalloys [8], ceramics [3], wood [9], composite materials [10] and others. Due to its wide application in industry, aluminum and its alloys are the subject of increased research, including regarding the possibilities of its laser processing [11].

The main characteristics of the laser texturing result are the width, the depth and the hatch. They can be determined directly experimentally by performing the laser texturing with the prescribed processing modes. To reduce setup time and the number of technological samples, computer models created on the basis of numerical methods, most often the finite element method (FEM), are applied. Commercial programs such as ABAQUS [9], [12], [13], COMSOL [14], [15], [16] and others are used for this purpose, as well as proprietary codes [5].

Most often, the modeling of laser texturing by the FEM to determine the resulting dimples is reduced to solving the problem of determining the temperature field by using the law of thermal conductivity. Regarding the considered area, the problem to be solved can be one-dimensional [13], two-dimensional [3], two-dimensional - axisymmetric [17] or three-dimensional [18], [9]. Depending on the number of set pulses, the models are for one pulse [9], for one transition [14] and several transitions [16]. A number of authors focus on the action of a single laser pulse [19], [5],

Print ISSN 1691-5402
Online ISSN 2256-070X
https://doi.org/10.17770/etr2023vol3.7278

which allows the determination of the temperature field, and from there the resulting topography.

The modeling of the processed part as a solid body is accomplished with Fourier's law. The heat flux can be volumetric or planarly distributed Gaussian function [16], [3]. Guo et al. [9] use in the heat flow's formula a coefficient considering the plasma. Nikolidakis et al. [16] also consider the influence of the evaporated plasma layer. Some authors consider radiation and convection [19], [8], but the process is fast and the heat conduction in the solid body has a dominant effect.

Some authors model the liquid phase by solving the Navier-Stokes equations [20]. This allows obtaining results for keyholes and voids in the material and splashes. Chryssolouris et al. [21] address the issue of plume formation. The evaporation at the melt surface is associated with the emission of neutral atoms or molecules into the gas that shields the laser–material interaction zone. Wang et al. [10] used in their work a simple finite element model to determine the plasma shielding effect in laser engraving of aluminum.

Computer determined crater dimensions can be used to validate the model. Liu et al. [22] offers a solution to the problem of measuring the diameter of such a small hole with a single laser pulse - D^2 method. In the modeling of laser texturing, in addition to the temperature field, some authors also determine the roughness of the obtained surfaces [15] and the stresses arising in the processing and after it [4], [3].

Numerical modeling of laser engraving can be performed by accounting for the nonlinear properties of the material [3]. A number of authors prefer the use of latent heat [20], which greatly eases the computational process.

The aim of the present research is the creation of a finite element model of laser texturing, allowing the determination of the groove width by taking into account the latent heat and the influence of the pulse power, the diameter of the laser beam, the reflection and the duration of the laser pulse.

II. Physical Laws Describing the Process

A complete physical description of the laser texturing process is difficult to achieve. This necessitates the use of a suitable physical-mathematical model, on the basis of which a computer model should be built, allowing the determination of the required quantities. For the needs of the presented study, it is assumed that the impact of the laser beam from the moment of its impact on the processed part, which is a solid body, will be considered.

The Fourier's law of heat conduction for solids is valid, which together with the heat balance equation has the form

$$\operatorname{div}\left(\mathbf{L}\cdot\operatorname{grad}(T)\right)+Q=\rho C_p\frac{\partial T}{\partial t}, \tag{1}$$

where **L** is the tensor with the heat transfer material characteristics depending on the temperature T, Q is the amount of heat in the considered volume, ρ is the density of the material C_p is the material heat capacity, and t is the time.

The laser beam is a flow of electromagnetic wave in the visible spectrum, which in the process of texturing propagates in the solid body according to the Beer-Lambert law [23]:

$$I(z)=I_0e^{-\alpha z}, \tag{2}$$

where $I(z)$ is the intensity at depth z and I_0 is the surface intensity. The equation for the absorption coefficient - α, is

$$\alpha=\frac{4\pi nk}{\lambda_0}, \tag{3}$$

where λ_0 is the wave length of the laser in vacuum, n is the refraction index, and k is the extinction index. The equations for the last characteristics are [24]:

$$n=\left(\frac{\sqrt{\varepsilon_1^2+\varepsilon_2^2}+\varepsilon_1}{2}\right)^{1/2}, \tag{4}$$

$$k=\left(\frac{\sqrt{\varepsilon_1^2+\varepsilon_2^2}-\varepsilon_1}{2}\right)^{1/2}, \tag{5}$$

where ε_1 and ε_2 are the real and the imagenery part of the material's relative permittivity.

Lehmuskero et al. [25] give their own and others' results for the refractive and absorption coefficients of aluminum. For a wavelength of 578 nm, n = 1 and k = 7 are reported. The same values are also used in [26].

Absorption is one of the parameters of the laser impact on the processed medium, as together with the reflection, R, give the heat flow vector [27]:

$$q=I(x,y)\left(1-R\right)e^{-\alpha z}, \tag{6}$$

The intensity of the laser beam depends on the power of the laser machine and is distributed according to a Gaussian law according to the equation

$$I(x,y)=\frac{2P_p}{\pi r^2}e^{-2\frac{\left(x-x_f\right)^2+\left(y-y_f\right)^2}{r^2}}, \tag{7}$$

where P_p is the pulse power of the laser, r is the radius of the laser beam, and x_f and y_f are the coordinates of the laser beam.

The phase changes from solid to liquid and from liquid to solid cause a strong nonlinearity in the specific heat capacity. In order to reduce the computational time, the latent heat is used, which is described by the equation

$$C_p = C_p^0 + L_m D_m + L_e D_e, \quad (8)$$

where C_p^0 is the equivalent specific heat capacity, L_m is the latent heat of melting, L_e is the latent heat of evaporation, and

$$D_m = \frac{\exp[-(T-T_m)^2/\Delta T_m^2]}{\Delta T_m \sqrt{\pi}}, \quad (9)$$

$$D_e = \frac{\exp[-(T-T_e)^2/\Delta T_e^2]}{\Delta T_e \sqrt{\pi}}, \quad (10)$$

In the above two equations take parts, the melting temperature - T_m, the evaporation temperature - T_e and the displacements relative to them - ΔT_m and ΔT_e.

III. Computer Model

The object of research is a part of pure aluminum subjected to laser processing. The process parameters ensure that a temperature above the vaporization temperature of aluminum is reached. Due to the small size of the diameter of the laser beam and the short duration of one pulse, a representative sample (Fig. 1) of the total volume of the body is considered. This has sufficient dimensions so that the physical laws can exhibit, and in the same time the dimensions to be small enough to minimize the duration of the computational process in the computer model. The dimensions of the representative volume are 100x100 μm in the processing plane and 70 μm in depth.

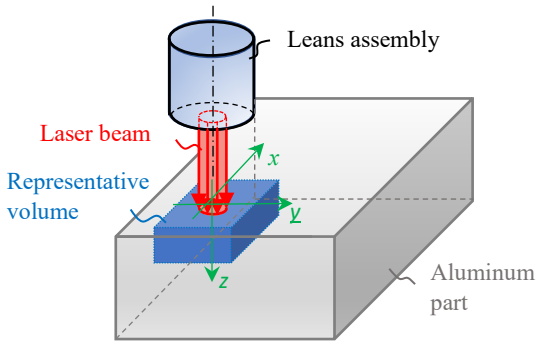

Fig. 1. General scheme of laser texturing.

The impact of a laser pulse, which creates a crater of a certain shape and size, is examined. The main properties of the crater are the width and the depth. In this work, it is accepted that the width is enough to characterize the result from the laser processing. It is based on the assumption that the formation of a groove consists of the repeated repetition of the pulse impact on the part, with the possibility of overlapping of individual craters and the presence of unprocessed areas - Fig. 2. The impact time between two pulses is long enough for the heat to spread in the considered representative volume and reach a temperature close to that of the environment at its boundaries. The formation of a complete processed layer is done by overlapping the furrows. Various processing sequences are possible to achieve such planar overlap, but these are beyond the scope of the present study. It is expedient to introduce an overlap factor between the individual craters in the direction of the groove

$$k = \frac{\nu d}{l_g} = \frac{\nu d}{vt}, \quad (11)$$

where ν is the pulse frequency and v is the speed of the laser.

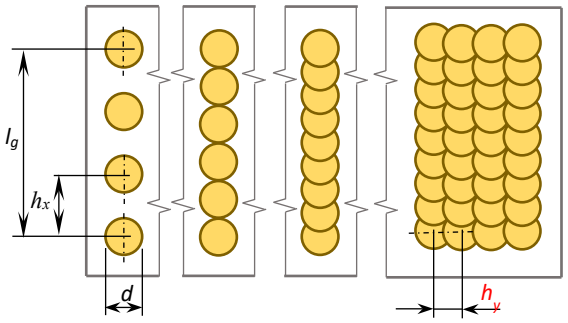

Fig. 2. Craters, grooves, layer.

A transient finite element model was created in the ABAQUS program [28]. Spatial discretization is performed using an eight-node hexahedral finite element DC3D8. The elements on the surface of laser impact are 1 μm in size - Fig. 3. To reduce the computational work, the feature size in the thickness direction is increased, reaching a size of 20 μm for the bottommost layer. The mesh is consist from 57222 nodes and 50500 elements.

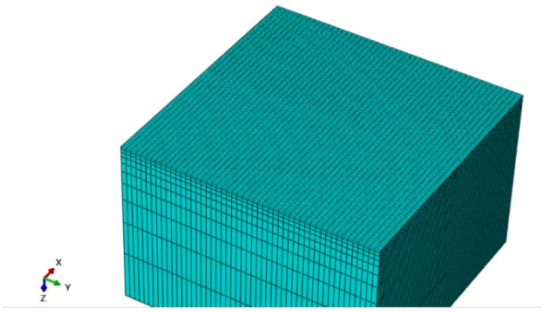

Fig. 3. Discretization of the representative volume.

The processed material is pure aluminum having the material characteristics given in Table 1. The liquid and gaseous phase changes are modeled by introducing latent heat (8), which allows the specific heat capacity to be set as constant.

Table 1 Material Properties

Material properties	Value
Density, kg/m^3	2700
Conductivity, W/(m.K)	235
Specific heat capacity, J/(kg.K)	900
Melting point, K	933,47

Material properties	Value
Evaporation temperature, K	2743
Latent heat of fusion, kJ/mol	10.71
Latent heat of vaporization, kJ/mol	284

It is assumed that the initial temperature of the test specimen is 20 °C. Convective and radiant heat transfer are neglected due to the short duration of the process. The time for one pulse – τ, is 30 μs. The pulse power is

$$P_p = P/\nu\tau, \qquad (12)$$

where P is the laser average power. Engraving modes with different laser power ranging from 5.5 to 10 W were investigated.

The laser beam is modeled as a heat flux equivalent to one pulse, according to (7). A volume distribution of the heat flux by means of a Gaussian function was used. The slope coefficient of the Gaussian function is taken to be equal to 3. The heat flux is specified in the model by subroutine DFLUX [28]. It allows setting the model characteristics that are involved in the parametric analysis: laser pulse power, focal diameter and reflection. The calculations were performed by discretizing the process time in 10000 increments.

IV. Results and Discussion

Temperature distribution results in a representative volume of a pure aluminum workpiece are obtained. In Fig. 4 shows the temperature field, at the end of the pulse, at a pulse power of 12511 W, a laser focal spot diameter of 30 μm and a reflection coefficient of 0.3.

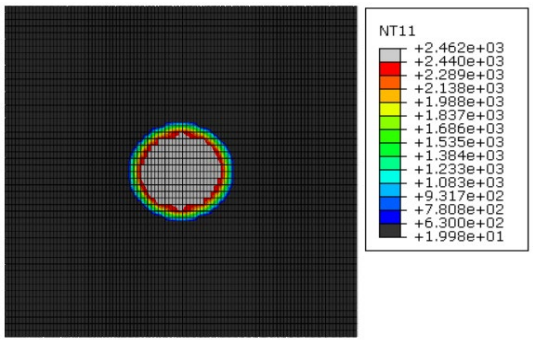

Fig. 4. Temperature distribution at P_p = 12511 W , d = 30 μm, R = 0.3.

The temperatures of the evaporation point are shown with a light color, and the temperatures below the melting point with a dark color. Similar diagrams are obtained for the different laser engraving modes. By measuring the evaporation isotherm, the width of the crater in the corresponding mode was obtained.

The effect of power density on crater width at two laser beam frequencies is shown in Fig. 5.

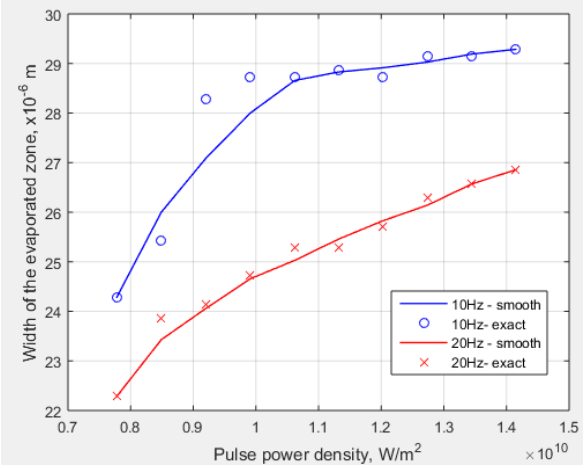

Fig. 5. Influence of pulse power density.

Figure 6 shows the dependences between the width of the vaporized zone - along the y axis and the pulse power - along the x axis. The resulting crater width results were smoothed using the smooth function in MATLAB, with the exact values given as dots. Such dependences were determined for focal spot diameters in the range from 10 to 30 μm, with a step of 5 μm.

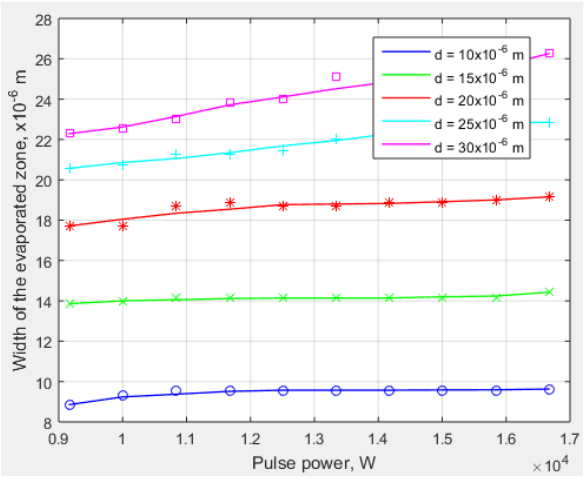

Fig. 6. Influence of pulse power on crater width at different focal spot diameters.

Increasing the pulse power leads to a smooth increase in the vaporized zone width. This trend is more distinct at larger values of the focal diameter.

The relationship between the reflection and the power at different diameters of the laser beam is shown at Fig. 7. The width of the crater decreases monotonically with increasing reflectivity. The effect of pulse power is linear.

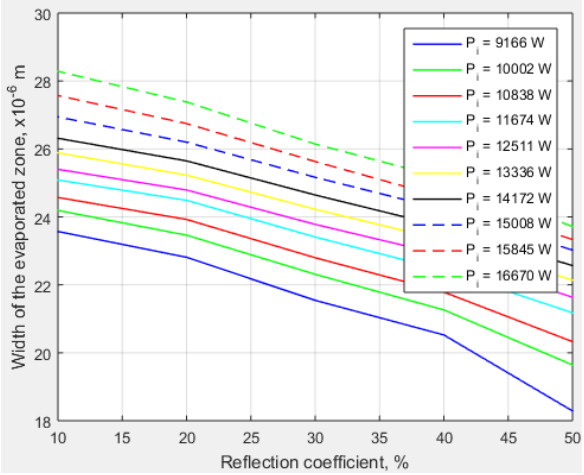

Fig. 7. Influence of the reflection.

Influence of the pulse duration on the width of the crater (Fig. 8) and the width of the molten zone – Fig 9.

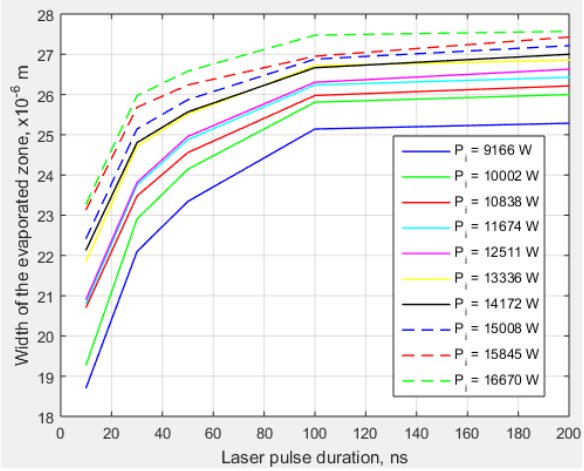

Fig. 8. Effect of pulse duration on crater width.

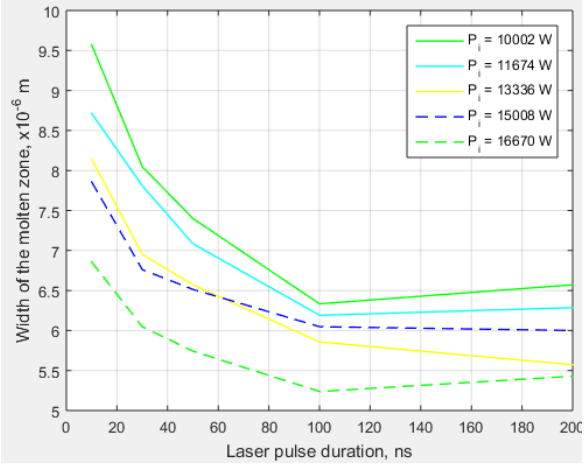

Fig. 9. Effect of pulse duration on the width of the melted zone.

It was found that as the pulse duration increased, the width of the vaporized zone increased. This tendency decreases for larger values of time. This parameter has a greater influence than the pulse power. The width of the melted zone, which contributes to the formation of irregularities, decreases with larger values of the laser pulse duration. For pulse durations above 100 ns, a tendency to increase the width is observed, which may be due to a numerical instability of the model related to the grid density.

The ablation threshold is the power density at which the evaporation temperature is reached. Ablation threshold at different laser pulse durations is shown in Fig. 10. The slope

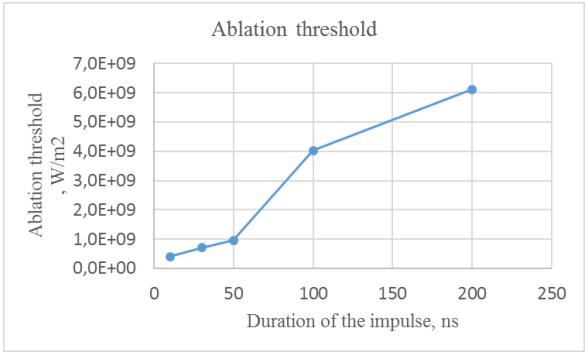

Fig. 10. Ablation threshold.

V. Conclusions

The created finite element model allows the determination of the influence of pulse power, reflection and diameter of the laser beam on the width of the vaporized zone during laser texturing of pure aluminum.

The pulse power has a linear effect on the width of the resulting craters. The influence of this parameter is less at small values of the diameter of the laser beam.

Increasing the reflectivity of the material leads to a decrease in the width of the crater. This trend is independent of the pulse power and increases with increasing reflection.

As the pulse duration increases, the width of the crater also increases. At larger values, this trend decreases, and above 100 ns it is particularly visible. The effect of pulse duration is inverse with respect to the width of the vaporized zone. At values above 100 ns, a trend reversal is observed, which may also be due to numerical instability. This question requires further research.

References

[1] D. Förster, B. Jëggi, A. Michalowski, B. Neuenschwander. Review on Experimental and Theoretical Investigations of Ultra-Short Pulsed Laser Ablation of Metals with Burst Pulses. Materials 14, 3331, 2021,
http://dx.doi.org/10.3390/ma14123331.

[2] A. Rosenkranz, P. Grützmacher, C. Gachot. H. Costa. Surface Texturing in Machine Elements – A Critical Discussion for Rolling and Sliding Contacts. Advanced Engineering Materials, 1900194, 2019,
http://dx.doi.org/10.1002/adem.201900194.

[3] S. Liu, Z. Tian, L. Shen, M. Qiu. Numerical Simulation and Experimental Investigation of Laser Ablation of Al2O3 Ceramic Coating. Materials 13, 5502, 2020,
http://dx.doi.org/10.3390/ma13235502.

[4] H. D. Vora, N. Dahotre. Multiphysics Theoretical Evaluation of Thermal Stresses in Laser Machined Structural Alumina. Laser Manuf. Mater. Process, 2:1-23, 2015,
http://dx.doi.org/10.1007/s40516-014-0004-x.

[5] L. Lazov, N. Angelov. Optimization of laser marking with the help of simulation models. Turkish Journal of Physics, 37, pp. 145-150, 2013,
http://dx.doi.org/10.3906/fiz-1202-4.

[6] T. Moriya, K. Fukumitsu, T. Yamashita, M. Watanabe. Fabrication of Finely Pitched LYSO Arrays Using Subsurface Laser Engraving Technique with Picosecond and Nanosecond Pulse Lasers. IEEE Transactions on nuclear science, Vol. 61, No. 2, pp. 1032-1037, 2014,
http://dx.doi.org/10.1109/TNS.2014.2309347.

[7] J. Lopez, F. Deloison, A. Lidolff, M. Delaigue, C. Hönninger, E. Mottay. Comparison of picosecond and femtosecond laser ablation for surface engraving of metals and semiconductors. Key Engineering Materials, Vol. 496, pp. 61-66, 2012,
http://dx.doi.org/10.1117/12.907792.

[8] B. Wang, Y. Huang, J. Jiao, H. Wang, J. Wang, W. Zhang, L. Sheng. Numerical Simulation on Pulsed Laser Ablation of the Single-Cristal Superalloy Considering Material Moving Front and Effect of Comprehensive Heat Dissipation. Micromachines, 12, 225, 2021,
http://dx.doi.org/10.3390/mi12020225.

[9] Q. Guo, Y. Ma, Z. Wu, Y. Cui, C. Yang. Finite Element Analysis and Experimental Research on Micro-treatment of Coniferous Wood Surface. Chemical Engineering Transactions, Vo. 55, pp. 91-96, 2016,
https://doi.org/10.3303/CET1655016.

[10] Y. Wang, D. W. Hahn. A simple element model to study the effect of plasma plume expansion on the nanosecond pulsed laser ablation aluminum. Applied Physics A, 125:654, 2019,
https://doi.org/10.1007/s00339-019-2951-8.

[11] M. Pantawane, S. Joshi, N. Dahotre. Laser Beam Machining of Aluminum and Aluminum Alloys. ASM Handbook, Vol. 2A, pp. 519-541, 2018,
http://dx.doi.org/10.31399/asm.hb.v02a.9781627082075.

[12] Y. Wang, O. Zhupanska, C. Pasiliao. Verification of a Manual Mesh Moving Finite Element Analysis Procedure for Modeling in Laminated Composite Materials. Proccedings of the ASME IMECE2017-70623, 2017,
http://dx.doi.org/10.1115/IMECE2017-70623.

[13] Y. Wang, T. Risch, C. Pasiliao. Modeling of Pyrolyzing Ablation Problem with ABAQUS: A One-Dimensional Test Case. Journal of Thermophysics and Heat Transfer, pp. 1-4, 2018,
http://dx.doi.org/10.2514/1.T5274.

[14] H. Karbasi. COMSOL Assisted Simulation of Laser Engraving. COMSOL Conference 2010 Boston, 2010.

[15] H. D. Vora, S. Santhanakrishnan, S. Harimkar, S. K. Boetcher, N. Dahotre. One-dimensional multipulse laser machining of structural alumina: evolution of surface topography. Int J Adv Manuf Technol 68, pp. 69-83, 2013,
https://doi.org/10.1007/s00170-012-4709-8.

[16] E. Nikolidakis, A. Antoniadis. FEM modeling simulation of laser engraving. The International Journal of Advanced Manufactoring Technology 105, pp. 3489–3498, 2019, https://doi.org/10.1007/s00170-019-04603-3.

[17] J. Kuang, T. Hung, K. Lai, C. Hsu, A. Lin. The Surface Absorption Coefficient of S304L Stainless Steel by Nd:YAG Micro-Pulse Laser. Advanced Material Research, Vol. 472-475, pp. 2531-3534, 2012,
http://dx.doi.org/10.4028/www.scientific.net/AMR.472-475.2531.

[18] H. D. Vora, N. Dahorte. Laser Machining of Structural Alumina: Influence of Moving Laser Beam on the Evolution of Surface Topography. Int. J. Appl. Ceram. Technol., pp. 1-14, 2014.

[19] H. D. Vora, S. Santhanakrishnan, S. Harimkar, S. Boetcher, N. Dahotre. Evolution of surface topography in one-dimensional laser machining of structural alumina. Journal of the European Ceramic Society 32, pp. 4205-4218, 2012,
http://dx.doi.org/10.1016/j.jeurceramsoc.2012.06.015.

[20] A. Otto, H. Koch, K. Leitz, M. Schmidt. Numerical Simulations – A Versatile Approach for Better Understanding Dynamics in Laser Material Processing. Physics Procedia 12, pp. 11-20, 2011,
http://dx.doi.org/10.1016/j.phpro.2011.03.003.

[21] G. Chryssolouris Laser machining theory and practice. New York: Springer- Verlag; 1991.

[22] J. Liu. Simple technique for measurements of pulsed Gaussian-beam spot sizes. Opt. Lett. **7**, pp. 196-198, 1982.

[23] M. Pantawane, S .Joshi, N. Dahotre. Laser Beam Machining of Aluminum and Aluminum Alloys. ASM Handbook, Vol. 2A, Aluminum Science and Technology, pp. 519-541, 2018,
http://dx.doi.org/10.31399/asm.hb.v02a.9781627082075.

[24] E. Beyer. Schweissen mit Laser, Berlin: Springer, pp. 28–36, 1995.

[25] A. M. Lehmuskero, M. Kuittinen, P. Vahimaa. Refractive index and extinction coefficient dependence of thin Al and Ir films on deposition technique and thickness. OPTICS EXPRESS, Vol. 15, No. 17, 2007,
http://dx.doi.org/10.1364/OE.15.010744.

[26] F. Hamadi, E. Amara, D. Bennaceur-Doumaz, R. Boutaka, H. Kellou, K. Bourai, A. Noukaz, R. Beggar. Modeling of Titanium Oxide Layer Growth Produces by Fiber Laser Beam. Defect and Diffusion Forum Vol. 336, pp. 11-18, 2013,
https://doi.org/10.4028/www.scientific.net/DDF.336.11.

[27] D. Bergström, A. Kaplan, J. Powell. Mathematical Modelling of Laser Absorption Mechanisms in Metals: A Review. M4PL16 - 16th Meeting on Mathematical Modelling of Materials Processing with Lasers, 2003.

[28] ABAQUS, "Analysis User's Manual," ver. 6.14, Dassault Systemes Simulia Corp., Providence, RI, USA.